

See discussions, stats, and author profiles for this publication at: <https://www.researchgate.net/publication/235650163>

# Regioselective Sequential Additions of Nucleophiles and Electrophiles to Perfluoroalkylfullerenes: Which Cage C Atoms Are the Most Reactive and Why?

ARTICLE *in* CHEMISTRY - A EUROPEAN JOURNAL · APRIL 2013

Impact Factor: 5.73 · DOI: 10.1002/chem.201203571 · Source: PubMed

CITATIONS

7

READS

58

7 AUTHORS, INCLUDING:



**Tyler T Clikeman**

Colorado State University

11 PUBLICATIONS 16 CITATIONS

SEE PROFILE



**Igor V Kuvychko**

Colorado State University

62 PUBLICATIONS 1,115 CITATIONS

SEE PROFILE



**Yu-Sheng Chen**

University of Chicago

121 PUBLICATIONS 1,463 CITATIONS

SEE PROFILE



**Alexey A Popov**

Leibniz Institute for Solid State and Materia...

188 PUBLICATIONS 3,381 CITATIONS

SEE PROFILE

# Regioselective Sequential Additions of Nucleophiles and Electrophiles to Perfluoroalkylfullerenes: Which Cage C Atoms Are the Most Reactive and Why?

Tyler T. Clikeman,<sup>[a]</sup> Igor V. Kuvychko,<sup>[a]</sup> Natalia B. Shustova,<sup>[a]</sup> Yu-Sheng Chen,<sup>[b]</sup> Alexey A. Popov,<sup>\*[c]</sup> Olga V. Boltalina,<sup>\*[a]</sup> and Steven H. Strauss<sup>\*[a]</sup>

**Abstract:** The sequential addition of  $\text{CN}^-$  or  $\text{CH}_3^-$  and electrophiles to three perfluoroalkylfullerenes (PFAFs),  $\text{C}_s\text{-C}_{70}(\text{CF}_3)_8$ ,  $\text{C}_{1-}\text{C}_{70}(\text{CF}_3)_{10}$ , and  $\text{C}_s\text{-}p\text{-C}_{60}(\text{CF}_3)_2$ , was carried out to determine the most reactive individual fullerene C atoms (as opposed to the most reactive C=C bonds, which has previously been studied). Each PFAF reacted with  $\text{CH}_3^-$  or  $\text{CN}^-$  to generate metastable  $\text{PFAF}(\text{CN})^-$  or  $\text{PFAF}(\text{CH}_3)_2^{2-}$  species with high regioselectivity

(i.e., one or two predominant isomers). They were treated with electrophiles  $\text{E}^+$  to generate  $\text{PFAF}(\text{CN})(\text{E})$  or  $\text{PFAF}(\text{CH}_3)_2(\text{E})_2$  derivatives, also with high regioselectivity ( $\text{E}^+ = \text{CN}^+$ ,  $\text{CH}_3^+$ , or  $\text{H}^+$ ). All of the predominant

products, characterized by mass spectrometry and  $^{19}\text{F}$  NMR spectroscopy, are new compounds. Some could be purified by HPLC to give single isomers. Two of them,  $\text{C}_{70}(\text{CF}_3)_8(\text{CN})_2$  and  $\text{C}_{70}(\text{CF}_3)_{10}(\text{CH}_3)_2(\text{CN})_2$ , were characterized by single-crystal X-ray diffraction. DFT calculations were used to propose whether a particular reaction is under kinetic or thermodynamic control.

**Keywords:** crystal-structure determination • density functional theory • fullerenes • perfluoroalkylfullerenes • regioselective synthesis

## Introduction

Fullerene derivatives are directly involved in the preparation of new materials for a wide variety of applications,<sup>[1]</sup> and perfluoroalkylfullerenes (PFAFs) are promising starting materials in this regard because they constitute one of the most diverse classes of derivatized fullerenes that exhibit high stability in air and in solution, thermal stability at elevated temperatures, and excellent solubility in organic solvents.<sup>[2–9]</sup> For example, there are more than 130 well-characterized fullerene( $\text{CF}_3$ )<sub>n</sub> compounds, including more than 30  $\text{C}_{60}(\text{CF}_3)_n$  derivatives.<sup>[2]</sup> For  $n=6, 8, 10$ , or  $12$ , the first reduc-

tion potentials for isomers of  $\text{C}_{60}(\text{CF}_3)_n$  vary by 0.33, 0.39, 0.50, or 0.48 V, respectively, and this wealth of structure/property information led to a detailed understanding of how different addition patterns affect the locations, shapes, and energies of fullerene-derivative frontier orbitals, and therefore how addition patterns affect, or might affect, physicochemical properties (an illustrative example is that two isomers of  $\text{C}_{60}(\text{CF}_3)_{10}$  that differ in the placement of only one  $\text{CF}_3$  group have first reduction potentials that differ by 0.40 V).<sup>[10]</sup>

Recent advances in synthetic methods and separation techniques have resulted in the availability of 100+ mg quantities of several PFAFs.<sup>[2,11]</sup> Rational, selective, and general further elaboration of PFAFs would allow this finely tuned set of molecules to be covalently linked to other functional molecules to afford supramolecular assemblies with a wide range of unique properties for specific applications. However, the current arsenal of PFAF derivatizations consists of only a few examples of two types of regioselective reactions: 1) cycloadditions to the C11–C29 bond in  $\text{C}_s\text{-}p^7\text{-C}_{70}(\text{CF}_3)_8$  (**I**)<sup>[12]</sup> and the C33–C34 bond in  $\text{C}_{1-}p^7mp\text{-C}_{70}(\text{CF}_3)_{10}$  (**II**)<sup>[13–15]</sup> and 2) the addition of two Cl atoms to **I**<sup>[16]</sup> and 12 Cl atoms to  $\text{S}_6\text{-C}_{60}(\text{CF}_3)_{12}$ .<sup>[17]</sup> Except for the 12-Cl-atom addition, these reactions allow 1) a single substituent (the exocyclic moiety) or 2) two identical radical substituents to be added to a particular C=C bond (i.e., to adjacent C atoms). A third reaction type, as yet unexplored for PFAFs, would consist of sequential additions of different substituents in a single reaction vessel, the addition of an anionic nucleophile followed by the addition of a cationic electro-

[a] T. T. Clikeman, Dr. I. V. Kuvychko, Dr. N. B. Shustova, Dr. O. V. Boltalina, Prof. S. H. Strauss  
Department of Chemistry, Colorado State University  
Fort Collins, CO 80523 (USA)  
Fax: (+1) 970-491-1801  
E-mail: olga.boltalina@colostate.edu  
steven.strauss@colostate.edu

[b] Dr. Y.-S. Chen  
ChemMatCARS Beamline  
University of Chicago Advanced Photon Source  
Argonne, IL 60439 (USA)

[c] Dr. A. A. Popov  
Department of Electrochemistry and Conducting Polymers  
Leibniz Institute for Solid State and Materials Research  
01069 Dresden (Germany)  
E-mail: a.popov@ifw-dresden.de

Supporting information for this article is available on the WWW under <http://dx.doi.org/10.1002/chem.201203571>.

phile, and these separate additions might not be to adjacent C atoms. To make the characterization of products and the determination of regioselectivity as straightforward as possible, an initial study of sequential nucleophile/electrophile additions to PFAFs with simple nucleophiles and electrophiles was initiated (again for simplicity, two of the electrophiles,  $\text{CN}^+$  and  $\text{CH}_3^+$ , have the same atomic composition as the two nucleophiles). We herein report that **I**, **II**, and  $\text{C}_s$ - $p\text{-C}_{60}(\text{CF}_3)_2$  (**III**) undergo regioselective addition of  $\text{CN}^-$  or  $\text{CH}_3^-$  and subsequent regioselective addition of  $\text{H}^+$  (i.e.,  $\text{CF}_3\text{COOH}$ ),  $\text{CH}_3^+$  (i.e.,  $\text{CF}_3\text{SO}_3\text{CH}_3$  ( $\text{CH}_3\text{OTf}$ )), or  $\text{CN}^+$  (i.e.,  $p\text{-TsCN}$ ).

## Results and Discussion

**General comments:** The purpose of this study was to determine which cage C atoms of a trio of fullerene derivatives are most susceptible to attack by anionic nucleophiles, and which cage C atoms of the anionic intermediates are most susceptible to attack by cationic electrophiles. There are two reasons why PFAFs are advantageous for such a study. The first is our experience with the synthesis, purification, and characterization of PFAFs.<sup>[2]</sup> The second, even more important advantage, is that, in many cases, the addition patterns of PFAFs and their derivatives can be readily determined by  $^{19}\text{F}$  NMR spectroscopy by virtue of through-space<sup>[5–7]</sup>  $J_{\text{FF}}$  spin–spin coupling between proximate  $\text{CF}_3$  groups and 2D  $^{19}\text{F}$  COSY correlations.<sup>[3,18–20]</sup> No other substituent X gives rise to multiple fullerene(X)<sub>n</sub> compositions and isomers and has the latter advantage.

Unlike previous studies that determined the C=C bonds most susceptible to cycloaddition for  $\text{C}_{60}$  derivatives<sup>[21–23]</sup> and for higher fullerenes,<sup>[22–25]</sup> we were interested in the reactivity of individual cage C atoms to nucleophilic and electrophilic attack. Would these C atoms belong to the most reactive C=C bonds? Even if they do, which of the two C=C atoms would react preferentially with the nucleophile? Would the electrophile then add to the second C atom of the original C=C bond or to a different cage C atom? And if it were possible to add two nucleophiles at the same time, where would the second nucleophile go? Presumably this would not be the second C atom of the original C=C bond.

Since our goal was not to synthesize specific derivatives that might have useful properties, many of the reactions we studied were on the NMR scale. For this reason, it was not possible to determine the yields of isolated compounds (i.e., the amounts were too small). In fact, some of the isomers identified were only generated in solution and were not isolated as pure compounds. Furthermore, since we were primarily interested in the addition patterns of the predominant isomers that were formed, we did not attempt to characterize isomers that were, based on  $^{19}\text{F}$  NMR spectroscopy, only present at  $\leq 5$  mol % yield.

Finally, we note that the seminal work of the groups of Wudl and Peel, which demonstrated that the strong nucleophile  $\text{CN}^-$  adds to  $\text{C}_{60}$  and to  $\text{C}_{60}(\text{CN})_2$  in solution<sup>[26,27]</sup> and

to  $\text{C}_{60}$ ,  $\text{C}_{70}$ , and a variety of higher fullerenes in the gas phase<sup>[28–30]</sup> and that  $p\text{-TsCN}$  reacts with  $\text{C}_{60}(\text{CN})_n^-$  to form  $\text{C}_{60}(\text{CN})_{n+1}$  ( $n=1, 3$ ),<sup>[26,27]</sup> provided the inspiration for this study.

**Reactions with  $\text{C}_s$ - $p^7\text{-C}_{70}(\text{CF}_3)_8$  (**I**):**  $^{19}\text{F}$  NMR spectra mentioned in this paragraph are shown in the Supporting Information. The addition of a colorless solution of  $\text{NET}_4\text{CN}$  in acetonitrile (MeCN) to a yellow solution of **I** in  $\text{C}_6\text{D}_6$  resulted in the immediate formation of a greyish-blue solution that exhibited an  $^{19}\text{F}$  NMR spectrum containing eight multiplets that was assigned to  $\text{C}_1\text{-C}_{70}(\text{CF}_3)_8(\text{CN})^-$  (the color of the solution persisted for at least 24 h). Subsequent addition of  $p\text{-TsCN}$  resulted in the formation of a brown solution containing an abundant derivative, **IV** (90+ mol % regioselectivity), that exhibited a  $^{19}\text{F}$  NMR spectrum with only four multiplets, which indicated  $\text{C}_s$  symmetry. A second isomer, present in approximately 10 mol % yield based on  $^{19}\text{F}$  NMR spectroscopy, was isolated and exhibited an eight-multiplet-containing spectrum, which indicated  $\text{C}_1$  symmetry. This is the first report of  $\text{CN}^-$  addition to a fullerene derivative other than Wudl's conversion of  $1,9\text{-C}_{60}(\text{CN})_2$  into five or more isomers of  $\text{C}_{60}(\text{CN})_4$  by using sequential  $\text{CN}^-$  and  $\text{CN}^+$  (i.e.,  $p\text{-TsCN}$ ) additions.<sup>[27]</sup>

X-ray crystallography<sup>[31]</sup> revealed that **IV** has the  $\text{C}_s$ - $p^9o$ -(loop) addition pattern shown in Figure 1. The  $p^9o$ -(loop) addition pattern was recently observed for  $\text{C}_{70}(\text{CF}_3)_8\text{Cl}_2$  (**V**);<sup>[16]</sup> it was first observed crystallographically for  $\text{C}_{70}\text{Br}_{10}$ .<sup>[32]</sup> In these derivatives, the C11–C29 bond (the only cage  $\text{C}(\text{sp}^3)\text{-C}(\text{sp}^3)$  bond) is long. It is 1.656(8), 1.63(1), and 1.59(2) Å in **IV**, **V**, and  $\text{C}_{70}\text{Br}_{10}$ , respectively. See the Supporting Information for a comparison of the structures of **IV** and **V**.

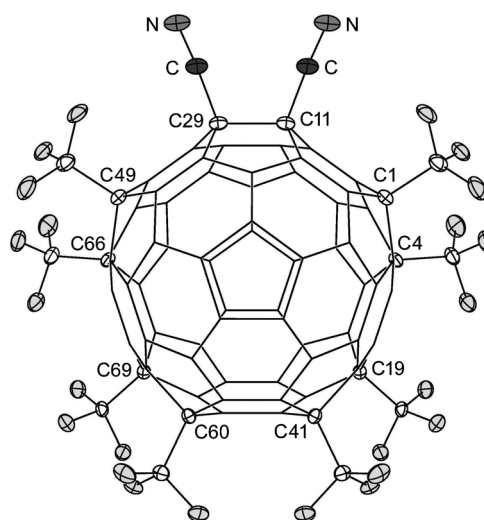


Figure 1. The structure of  $\text{C}_s$ - $p^9o$ -(loop)- $\text{C}_{70}(\text{CF}_3)_8(\text{CN})_2$  (**IV**), showing ellipsoids at the 50% probability level for the ten substituents and the cage C atoms to which they are attached (disordered  $\text{CHCl}_3/\text{CH}_2\text{Cl}_2$  molecules are omitted; only half of the molecule is unique (i.e.,  $\text{C}_{29}=\text{C}_{11}'$ ,  $\text{C}_{49}=\text{C}_{1'}$ , etc.)). Selected distances [Å] and angles [°]: C11–CN 1.476(5), C–N 1.145(5), C11–C29 1.658(8); C11–C–N 177.0(4), C11–C29–C 110.7(2).

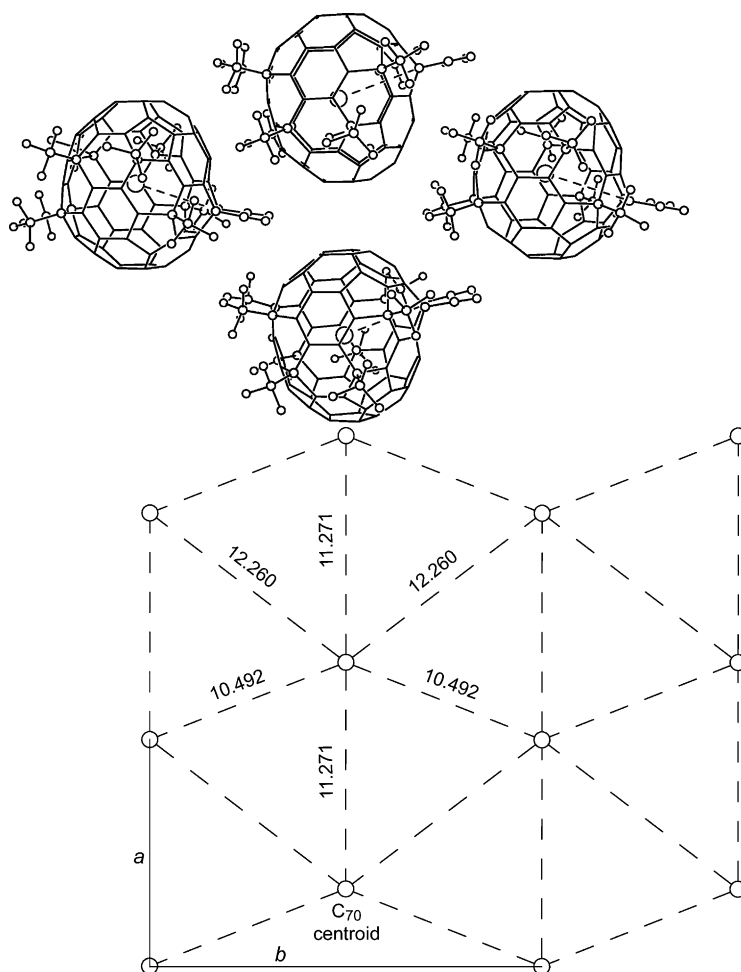


Figure 2. The packing of molecules of **IV** in rigorously planar pseudohexagonal layers of  $C_{70}$  centroids ( $\odot$ , large circles, this is the crystallographic  $ab$  plane). The  $\odot \cdots \odot$  distances shown in the lower drawing are in Å. In the upper drawing, which is shown in the same orientation as the lower drawing, ----- connect the  $C_{70}$  centroids with the centroids of the C11–C29 bonds, which are approximately the same as the directions of the molecular dipole vectors. The dipole vectors have the same crystallographic  $b$  components, with offsetting components along the crystallographic  $a$  axis.

The DFT-predicted dipole moment of **IV** is 4.59 D. The DFT-predicted dipole moments of **I** (1.65 D) and **V** (0.75 D) are much smaller. In fact, the dipole moments of **I** and **IV** point in opposite directions, which demonstrates the potential for significantly changing the properties of PFAFs by judicious regioselective additions (see the Supporting Information for more details about the dipole moments of **I**, **IV**, and **V**). Not surprisingly, the large dipole moment of **IV** leads to an interesting three-dimensional packing of molecules in the solid state. Figure 2 shows the packing in one layer in the crystal lattice (the disordered solvent molecules have been omitted for clarity).

The  $C_{70}$  cage centroids,  $\odot$ , form rigorously planar pseudohexagonal arrays in crystallographic  $ab$  planes with  $\odot \cdots \odot$  distances within each layer that range from 10.492 to 12.260 Å. These layers are stacked in the crystallographic  $c$  direction with 13.173 Å spacings, resulting in the pseudo-HCP packing shown in Figure 3. Within each layer the molecular dipole vectors have the same  $b$  component, and al-

ternate strongly dipolar layers have their resultant dipole vectors in the  $+b$  or  $-b$  direction.

Figure 4 shows the IUPAC numbering for  $C_{70}$ , the DFT-predicted LUMO of **I**, and a DFT-predicted electrostatic potential (ESP) diagram for the  $C_{70}(CF_3)_8(CN)^-$  isomer with its CN group on C11. It is virtually certain that the predominant  $C_{70}(CF_3)_8(CN)^-$  isomer is the 11-CN isomer because the predominant product, **IV**, has CN groups on C11 and C29 (note that C11 and C29 are symmetry related in **I**). The DFT calculations listed in Table 1 show that the 11-CN anion is favored by 7.6 kJ mol $^{-1}$  over the next most stable isomer, with the CN group on C25. In addition, nucleophilic attack on C11 in **I** is also favored due to the large contributions of p- $\pi$  orbitals on C11 (and C29) to the LUMO of **I**. The PFAF **I**, with its  $C_s$ - $p^7$  addition pattern, is unusual in that the addition of two Cl atoms initiated by the ICl electrophilic (or radical) attack, and the addition of two CN groups initiated by  $CN^-$  nucleophilic attack both lead to a  $C_s$ - $p^9o(loop)$  isomer as the abundant product. This is because both the HOMO and the

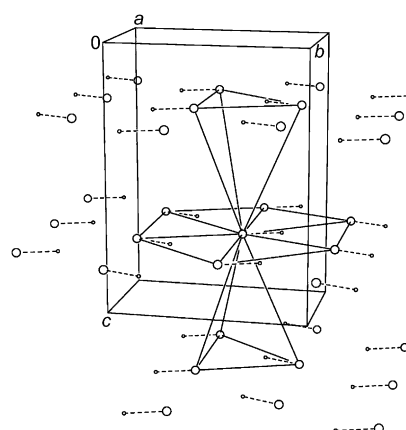


Figure 3. The stacking of planes of **IV** in the crystallographic  $c$  direction. ----- connect the  $C_{70}$  centroids with the centroids of the C11–C29 bonds, and these are approximately the same as the directions of the molecular dipole vectors.



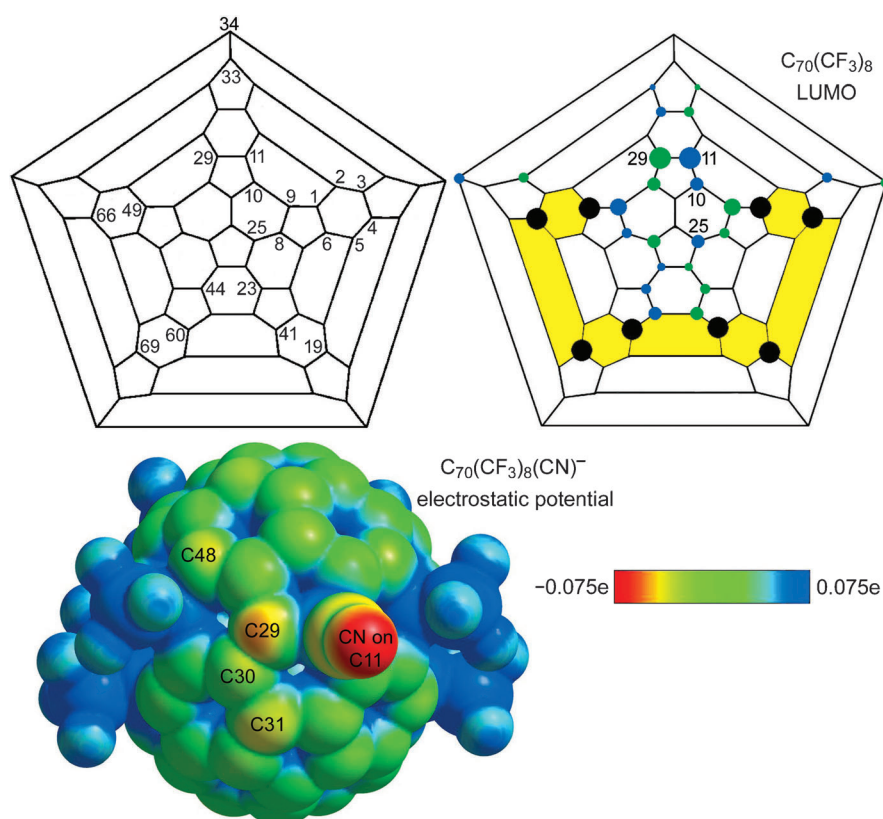


Figure 4. The IUPAC numbering for C<sub>70</sub>, the DFT-predicted LUMO for C<sub>s</sub>-p<sup>7</sup>-C<sub>70</sub>(CF<sub>3</sub>)<sub>8</sub> (**I**), and a DFT-predicted ESP diagram for C<sub>s</sub>-p<sup>8</sup>-C<sub>70</sub>(CF<sub>3</sub>)<sub>8</sub>(CN)<sub>2</sub><sup>-</sup>. The p-π orbital contributions to the LUMO, shown as green or blue circles, are approximately proportional in size to their relative contributions to the orbital.

Table 1. DFT-predicted relative energies (kJ mol<sup>-1</sup>) of selected C<sub>70</sub>(CF<sub>3</sub>)<sub>8</sub>(CN)<sup>-</sup> anions and neutral C<sub>70</sub>(CF<sub>3</sub>)<sub>8</sub>(CN)<sub>2</sub> compounds.<sup>[a]</sup>

CN locant	ΔE (anion)	2nd CN locant	ΔE (neutral) <sup>[c]</sup>
11	0.0	29	0.0
11		31	44.9
11		48	56.9
11		30	220.5
25	7.6	10	42.6
9	13.5		
34	20.3		
23	25.8		

[a] The locants refer to the numbered Schlegel diagram in Figure 5.

LUMO of **I** have large contributions from the p-π orbitals on C11 and C29.

The ESP for the 11-CN isomer of C<sub>70</sub>(CF<sub>3</sub>)<sub>8</sub>(CN)<sup>-</sup>, mapped onto its van der Waals surface, indicates that the cage C atoms with the greatest negative charge are C29 and C31, which should be the two sites favored for electrophilic attack by p-TsCN. Combined with the results in Table 1, CN<sup>+</sup> addition to C29 is favored relative to any other cage C atom. This explains the formation of the major C<sub>s</sub> isomer **IV**. If minor isomer C<sub>1</sub>-C<sub>70</sub>(CF<sub>3</sub>)<sub>8</sub>(CN)<sub>2</sub> is formed from the minor 25-CN isomer of C<sub>70</sub>(CF<sub>3</sub>)<sub>8</sub>(CN)<sup>-</sup> (7.6 kJ mol<sup>-1</sup> less stable than the 11-CN isomer), then the most likely addition pattern of C<sub>1</sub>-C<sub>70</sub>(CF<sub>3</sub>)<sub>8</sub>(CN)<sub>2</sub> is the C<sub>1</sub>-p<sup>7</sup>mp addition pattern, with CN groups on C10 and C25. Interestingly, C<sub>1</sub>-

p<sup>7</sup>mp-C<sub>70</sub>(CF<sub>3</sub>)<sub>10</sub> (**II**), the lowest-energy isomer of C<sub>70</sub>(CF<sub>3</sub>)<sub>10</sub>, is predicted to be only 12.4 kJ mol<sup>-1</sup> lower in energy than the putative isomer C<sub>s</sub>-p<sup>9</sup>o(loop)-C<sub>70</sub>(CF<sub>3</sub>)<sub>10</sub>, whereas **IV** is predicted to be 42.6 kJ mol<sup>-1</sup> lower in energy than C<sub>1</sub>-p<sup>7</sup>mp-C<sub>70</sub>(CF<sub>3</sub>)<sub>8</sub>(CN)<sub>2</sub>. The small difference in DFT-predicted energies for **II** and C<sub>s</sub>-p<sup>9</sup>o(loop)-C<sub>70</sub>(CF<sub>3</sub>)<sub>10</sub> is clearly due to the large size of CF<sub>3</sub> substituents, since we have also found that the hypothetical isomer C<sub>s</sub>-p<sup>9</sup>o(loop)-C<sub>70</sub>H<sub>10</sub> is 47.1 kJ mol<sup>-1</sup> lower in energy than the hypothetical isomer C<sub>1</sub>-p<sup>7</sup>mp-C<sub>70</sub>H<sub>10</sub>.

Another possibility is that the minor isomer derives from CN<sup>+</sup> addition to C31 of the 11-CN isomer of C<sub>70</sub>(CF<sub>3</sub>)<sub>8</sub>(CN)<sup>-</sup>. This would produce a C<sub>1</sub>-p<sup>9</sup>-isomer of C<sub>70</sub>(CF<sub>3</sub>)<sub>8</sub>(CN)<sub>2</sub>, an addition pattern known for two symmetric C<sub>70</sub>X<sub>10</sub> compounds, C<sub>2</sub>-p<sup>9</sup>-C<sub>70</sub>(CF<sub>3</sub>)<sub>10</sub><sup>[33]</sup> and C<sub>2</sub>-p<sup>9</sup>-C<sub>70</sub>(tBuOO)<sub>10</sub><sup>[34]</sup>. However, the UV/Vis spectrum of the minor isomer is nearly congruent

with the spectrum of C<sub>1</sub>-p<sup>7</sup>mp-C<sub>70</sub>(CF<sub>3</sub>)<sub>10</sub> (**II**) and significantly different than the spectrum of C<sub>2</sub>-p<sup>9</sup>-C<sub>70</sub>(CF<sub>3</sub>)<sub>10</sub> (these spectra are shown in the Supporting Information). Therefore, we conclude that the minor isomer is most likely C<sub>1</sub>-p<sup>7</sup>mp-C<sub>70</sub>(CF<sub>3</sub>)<sub>8</sub>(CN)<sub>2</sub>, formed from the 25-CN minor isomer of C<sub>70</sub>(CF<sub>3</sub>)<sub>8</sub>(CN)<sup>-</sup>. Note that this is an example of a pair of substituents being added to the *para* positions of a cage hexagon instead of a cage C=C bond, even though the addition of the same substituents to a cage C=C is possible (and in fact, in this case, represents the more abundant product).

**Reactions with C<sub>1</sub>-p<sup>7</sup>mp-C<sub>70</sub>(CF<sub>3</sub>)<sub>10</sub> (**II**):** Rather than pursuing additional reactions with **I**, we turned our attention to **II**, an asymmetric compound with 60 unique C(sp<sup>2</sup>) atoms to which a nucleophile might add. Addition of a solution of NEt<sub>4</sub>CN in MeCN to a yellow solution of **II** in C<sub>6</sub>D<sub>6</sub>/PhCH<sub>3</sub> resulted in the immediate formation of a green species with a new set of 10 CF<sub>3</sub> multiplets in the <sup>19</sup>F NMR spectrum shown in Figure 5 (95+mol% regioselectivity based on NMR spectroscopy). Subsequent addition of CH<sub>3</sub>OTf or CF<sub>3</sub>COOH resulted in the immediate formation of yellow solutions containing, in either case, a major product also with 95+mol% regioselectivity based on their NMR spectra. These were purified by HPLC and exhibited nearly identical <sup>19</sup>F NMR spectra, which suggested identical addition patterns.

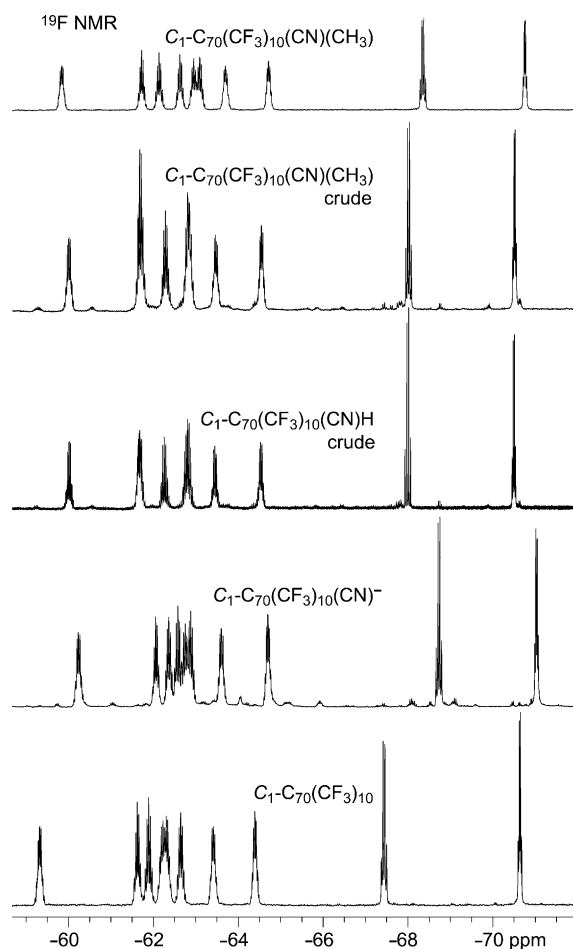


Figure 5.  $^{19}\text{F}$  NMR spectra (2:2:1  $\text{C}_6\text{D}_6/\text{PhCH}_3/\text{MeCN}$ , 376.5 MHz,  $\delta-(\text{C}_6\text{F}_6) = -164.9$  ppm) showing (bottom to top) the ten multiplets for **II**,  $\text{C}_{70}(\text{CF}_3)_{10}(\text{CN})^-$  (95+mol% regioselectivity),  $\text{C}_{70}(\text{CF}_3)_{10}(\text{CN})(\text{H})$  and  $\text{C}_{70}(\text{CF}_3)_{10}(\text{CN})(\text{CH}_3)$  crude reaction products (both with 90+mol% regioselectivity), and purified  $\text{C}_{70}(\text{CF}_3)_{10}(\text{CN})(\text{CH}_3)$  (in  $\text{C}_6\text{D}_6$ ).

DFT calculations suggest that the  $\text{C}_{70}(\text{CF}_3)_{10}(\text{CN})^-$  intermediate probably has its CN group on C34, as shown in Table 2 and Figure 6, although the preference for this site is only 6.6  $\text{kJ mol}^{-1}$ . Based on the p- $\pi$  orbital contributions to the LUMO and LUMO+1 of **II**, the sites favored for nucleophilic attack by  $\text{CN}^-$  on  $\text{C}_{1-p^7mp}\text{-C}_{70}(\text{CF}_3)_{10}$  may be C33 and C34, followed by C29 and C11 (which are sterically crowded because they share a pentagon or a pentagon and a hexagon, respectively, with  $\text{CF}_3$  groups). The LUMO in Figure 6 is based on figures published in 2008;<sup>[13,33]</sup> the LUMO+1 diagram appears here for the first time. Although LUMO+2 is only 0.04 eV above LUMO+1, it is not shown because the same cage C atoms are involved. Therefore, the remarkably selective nucleophilic addition of  $\text{CN}^-$  to **II** may be under kinetic and thermodynamic control, because all of the other low-energy  $\text{CN}^-$  addition sites (except C33), not just C11 and C29, share a pentagon or a pentagon and a hexagon with bulky  $\text{CF}_3$  groups.

If the CN group is indeed on C34 in  $\text{C}_{70}(\text{CF}_3)_{10}(\text{CN})^-$ , then the product with its  $\text{CH}_3$  group on C33 (i.e.,  $\text{C}_{70}(\text{CF}_3)_{10}$ -

Table 2. DFT-predicted relative energies ( $\text{kJ mol}^{-1}$ ) of selected  $\text{C}_{70}(\text{CF}_3)_{10}(\text{CN})^-$  anions and neutral  $\text{C}_{70}(\text{CF}_3)_{10}(\text{CN})(\text{CH}_3)$  compounds.<sup>[a]</sup>

CN locant	$\Delta E$ (anion)	$\text{CH}_3$ locant	$\Delta E$ (neutral)
34	0.0	33	0.0
34		15	46.6
34		52	49.0
34		13	80.9
34		31	92.2
53	6.6	33	30.7
16	7.8	33	32.7
33	9.5	34	1.0
33		53	30.9
33		16	32.6
37	13.3		
11	14.1		
15	14.5		
44	15.1	23	12.0
56	15.6		
29	16.7		
52	16.8		

[a] The locants refer to the numbered Schlegel diagram in Figure 5.

(34-CN)(33- $\text{CH}_3$ )) may also be kinetically and thermodynamically favored: kinetically according to the ESP for  $\text{C}_{70}(\text{CF}_3)_{10}(\text{CN})^-$  shown in Figure 6 and the fact that all other cage C atoms share a pentagon with a  $\text{CF}_3$  group, and thermodynamically by more than 46  $\text{kJ mol}^{-1}$ . Note that there is only a 1.0  $\text{kJ mol}^{-1}$  difference in the DFT-predicted energies of  $\text{C}_{70}(\text{CF}_3)_{10}(34\text{-CN})(33\text{-CH}_3)$  and  $\text{C}_{70}(\text{CF}_3)_{10}(33\text{-CN})(34\text{-CH}_3)$ .

The  $\text{C}_{70}(\text{CF}_3)_{10}(44\text{-CN})(23\text{-CH}_3)$  isomer can be dismissed as a candidate for the predominant isomer despite the fact that the X-ray structure of  $\text{C}_{70}(\text{CF}_3)_{10}(\text{CH}_3)_2(\text{CN})_2$ , which will be discussed below, shows that a nucleophile/electrophile pair can add to C44 and C23, respectively, on **II** (note that these cage C atoms are *para* to one another on a hexagon near the  $\text{C}_{70}$  equator, whereas the C33–C34 bond is near one of the  $\text{C}_{70}$  poles). The DFT-predicted energies of  $\text{C}_{70}(\text{CF}_3)_{10}(44\text{-CN})^-$  and  $\text{C}_{70}(\text{CF}_3)_{10}(44\text{-CN})(23\text{-CH}_3)$  are 15.1 and 12.0  $\text{kJ mol}^{-1}$  higher, respectively, than the corresponding lowest-energy isomers. In addition to the steric hindrance at C44 relative to C34, the  $^{19}\text{F}$  NMR spectrum of the 95+mol% regioselective product does not exhibit a pair of multiplets with  $-\delta$  values  $\leq 60$ , which suggests that the added substituents have not affected the conformations of the  $\text{CF}_3$  groups relative to the conformations observed for **II** and therefore are remote from the  $\text{CF}_3$  groups (see the NMR spectra for  $\text{C}_{70}(\text{CF}_3)_{10}(\text{CH}_3)_2(\text{CN})_2$  in the Supporting Information).<sup>[3,18,35]</sup> Considering all of the experimental and DFT results, we conclude that the predominant products formed by treating **II** first with  $\text{NEt}_4\text{CN}$  and then with either  $\text{CH}_3\text{OTf}$  or  $\text{CF}_3\text{COOH}$  are  $\text{C}_{70}(\text{CF}_3)_{10}(34\text{-CN})(33\text{-CH}_3)$  and  $\text{C}_{70}(\text{CF}_3)_{10}(34\text{-CN})(33\text{-H})$ , respectively.

We explored the possibility of generating the “opposite isomer”  $\text{C}_{70}(\text{CF}_3)_{10}(34\text{-CH}_3)(33\text{-CN})$  by first adding  $\text{CH}_3^-$  (as  $\text{LiCH}_3$ ) followed by  $p\text{-TsCN}$ . As explained below, this could not be accomplished, but this strategy led to an important discovery. Since MeCN cannot be used with  $\text{LiCH}_3$ , a solution of  $\text{LiCH}_3$  in  $\text{Et}_2\text{O}$  was added to a solution of **II** in

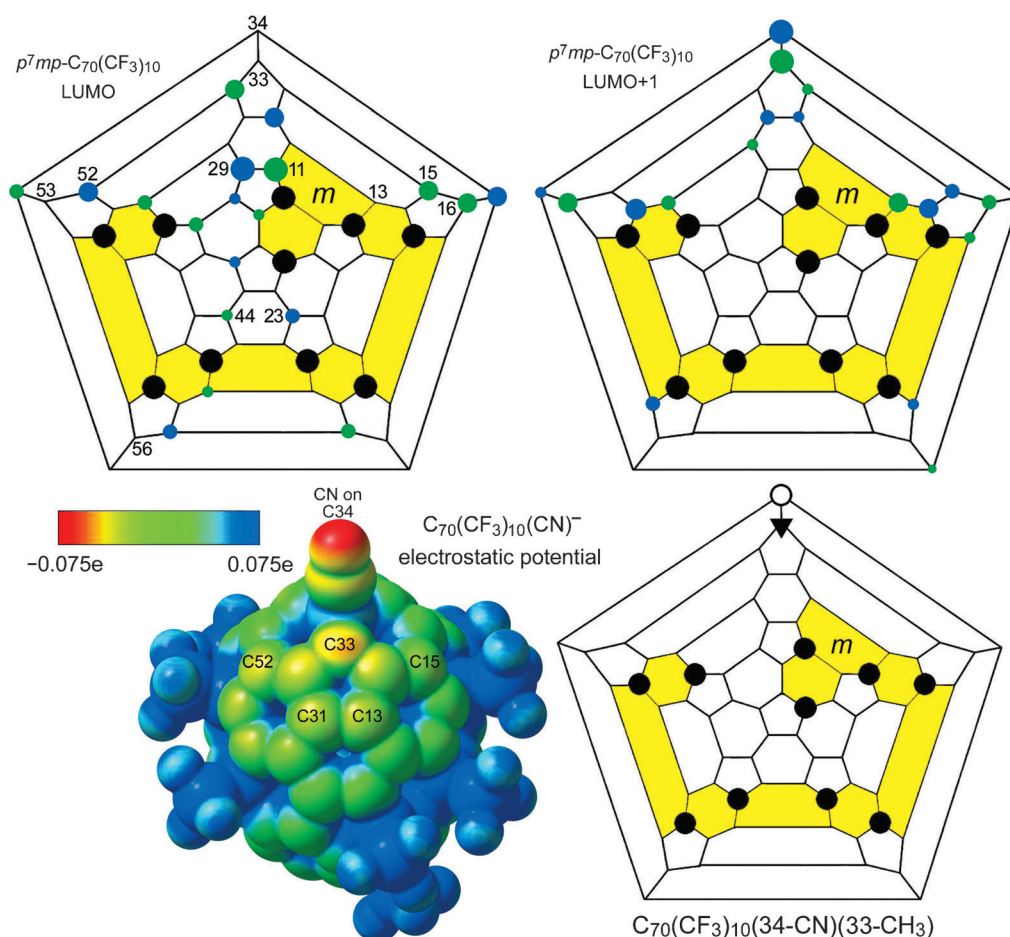


Figure 6. Schlegel diagrams showing the DFT-predicted LUMO and LUMO+1 for  $C_{1-p^7mp-C_{70}(CF_3)_{10}}$  (**II**, top), a DFT-predicted ESP diagram for  $C_{1-p^7mp-C_{70}(CF_3)_{10}(CN)^-}$ , and the Schlegel diagram for the most likely isomer of  $C_{1-p^7mp-C_{70}(CF_3)_{10}(CN)(CH_3)}$  with its CN group ( $\circ$ ) and  $CH_3$  group ( $\blacktriangledown$ ) on C34 and C33, respectively.

PhCH<sub>3</sub>. A green precipitate formed immediately when the two solutions were mixed. When only one or two equivalents of LiCH<sub>3</sub> were added, an <sup>19</sup>F NMR spectrum (broadened by the presence of the green precipitate; see the Supporting Information) indicated that some amount of **II** was still present in solution. Four equivalents of LiCH<sub>3</sub> were required to cause the complete conversion of yellow, soluble **II** into the green precipitate, presumably the lithium salt of a putative  $C_{70}(CF_3)_{10}(CH_3)_n^{n-}$  anion. Subsequent addition of four equivalents of *p*-TsCN dissolved in PhCH<sub>3</sub> caused the immediate conversion of the green precipitate into a yellow solution.

The <sup>19</sup>F NMR spectrum of the yellow solution (Supporting Information) indicated the absence of **II** and the presence of two principal products, one of them more abundant than the other. These two products were purified by HPLC (confirming their different relative abundances) and exhibited the NMR spectra also shown in the Supporting Information. Mass spectra showed that they were isomers of the composition  $C_{70}(CF_3)_{10}(CH_3)_2(CN)_2$ . It is unlikely that the green precipitate only contained the  $C_{70}(CF_3)_{10}(CH_3)^-$  monoanion and that the excess LiCH<sub>3</sub> present in solution added to  $C_{70}$ -

$(CF_3)_{10}(CH_3)(CN)$  as it formed from the green solid when *p*-TsCN was added, because free LiCH<sub>3</sub> reacts extremely rapidly with *p*-TsCN to form CH<sub>3</sub>CN (i.e., there would be little or no remaining LiCH<sub>3</sub> to react with the putative intermediate  $C_{70}(CF_3)_{10}(CH_3)(CN)$ ). Therefore, we propose that the green precipitate contains two (or more) isomers of the lithium salt of the  $C_{70}(CF_3)_{10}(CH_3)_2^{2-}$  dianion, namely the dianions that form the major and minor isomers of  $C_{70}(CF_3)_{10}-(CH_3)_2(CN)_2$ .

The minor isomer formed crystals suitable for X-ray diffraction, and its structure is shown in Figure 7<sup>[36]</sup> (the structure is of poor quality, with an *R<sub>w</sub>* value of 0.21, but there is no doubt about its addition pattern, which is the only feature of the structure that is relevant to this paper; see the Supporting Information for more details). The two CH<sub>3</sub> groups have been added to C33 and C44; the two CN groups have been added to C34 and C23. It was expected that a nucleophile/electrophile pair would add to the C33–C34 bond (although in this isomer the two groups are switched from the proposed, lowest-energy isomer  $C_{70}-(CF_3)_{10}(34-CN)(33-CH_3)$ ). The other nucleophile/electrophile pair have been added to the *para* positions of a hexagon



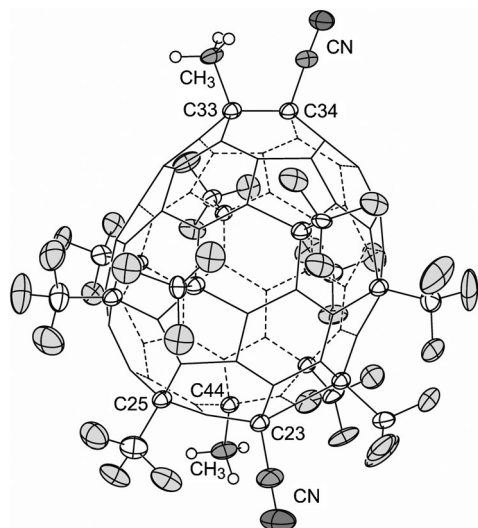


Figure 7. The structure of minor isomer  $C_1-C_{70}(CF_3)_{10}(33,44-CH_3)_2(23,34-CN)_2$  (50% probability ellipsoids for the 14 substituents and the C atoms to which they are attached, H atoms shown as spheres of arbitrary size,  $CH_2Cl_2$  solvent omitted for clarity).

near the  $C_{70}$  equator. The presence of both  $C_s-p^o(\text{loop})-C_{70}(CF_3)_8(CN)_2$  and  $C_1-p^7mp-C_{70}(CF_3)_8(CN)_2$  resulting from the addition of  $CN^-$  and  $CN^+$  to **I** showed that a nucleophile/electrophile pair can add to a cage C=C bond or to the *para* positions of a cage hexagon. The formation of  $C_{70}(CF_3)_{10}(33,44-CH_3)_2(23,34-CN)_2$  shows that both types of addition can occur simultaneously on the same substrate molecule.

It is likely that the minor isomer characterized by X-ray diffraction was formed by the addition of two  $CN^+$  moieties to the  $C_{70}(CF_3)_{10}(33,44-CH_3)_2^{2-}$  dianion. DFT calculations, listed in Table 3, predict that this isomer is 4.1 kJ mol $^{-1}$  less

Table 3. DFT-predicted relative energies (kJ mol $^{-1}$ ) of selected  $C_{70}(CF_3)_{10}(CH_3)_2^{2-}$  dianions and neutral  $C_{70}(CF_3)_{10}(CH_3)_2(CN)_2$  compounds.<sup>[a]</sup>

CN locants	$\Delta E$ (dianion)	CH <sub>3</sub> locants	$\Delta E$ (neutral)
34, 44	0.0	23, 33	0.8
33, 44	4.1	23, 34	0.0
33, 23	37.7	52	2.5
33, 34	75.7	–	–

[a] The locants refer to the numbered Schlegel diagram in Figure 5.

stable than the corresponding  $(34,44-CH_3)_2$  dianion. Based on the DFT predictions, and the near congruence of the  $^{19}F$  NMR spectra of the major and minor isomers, it seems likely that the major isomer was formed from the  $C_{70}(CF_3)_{10}(34,44-CH_3)_2^{2-}$  dianion and is  $C_1-C_{70}(CF_3)_{10}(34,44-CH_3)_2(23,33-CN)_2$  (note that both isomers exhibit two multiplets with  $-\delta$  values  $\leq 60$  ppm, which indicates that the added substituents have affected the conformation of one  $CF_3$  group relative to its conformation in **II**). Both the X-ray structure and the DFT-optimized structure of the minor isomer show that the 23-CN and 44- $CH_3$  substituents are in

close proximity to two  $CF_3$  groups and one  $CF_3$  group, respectively (see the Supporting Information). The multiplet at  $\delta = -61.6$  ppm in the spectrum of **II** belongs to the  $CF_3$  group closest to the  $CH_3$  group on C44.<sup>[18]</sup> It is sensible that this multiplet would be the one to shift to approximately  $\delta = -58$  ppm in the spectra of  $C_{70}(CF_3)_{10}(CH_3)_2(CN)_2$ . Furthermore, note that the quartet at  $\delta = -70.9$  ppm in the spectrum of **II** also experiences a large shift. This is because the terminal  $CF_3$  group on C25 in **II** is no longer terminal in  $C_{70}(CF_3)_{10}(CH_3)_2(CN)_2$ ; it is *para* to the  $CF_3$  group on C10 and *meta* to the CN group on C23.

Interestingly, the minor isomer is predicted to be marginally more stable than the major isomer, not less stable. The calculations also predict that the addition of one of the two  $CH_3^-$  nucleophiles to C23, or the addition of both of them to C33 and C34, are unlikely. An ESP diagram of the  $C_{70}(CF_3)_{10}(33,44-CH_3)_2^{2-}$  dianion shows that the addition of  $CN^+$  electrophiles to C34 and C23 may be kinetically controlled and thermodynamically favored. In addition,  $C_{70}(CF_3)_{10}(33,44-CH_3)_2(34-CN)^-$  and  $C_{70}(CF_3)_{10}(33,44-CH_3)_2(23-CN)^-$  ESP diagrams show that the addition of  $CN^+$  to C23 or C34, respectively, may also be kinetically controlled.

**Reactions with  $C_s-p-C_{60}(CF_3)_2$  (**III**):** Addition of a solution of  $NEt_4CN$  in  $CH_2Cl_2$  to a brown solution of **III** in  $CH_2Cl_2$  resulted in the formation of a brown species that exhibited a two-quartet-containing  $^{19}F$  NMR spectrum consistent with  $C_1$  symmetry and 95+ mol% regioselectivity, as shown in Figure 8B. Subsequent addition of  $CH_3OTf$  or  $CF_3COOH$  resulted in the immediate formation of orange solutions containing, in either case, two predominant isomers of  $C_1-C_{60}(CF_3)_2(CN)(X)$  ( $X = CH_3$  or  $H$ , respectively). DFT calculations suggest that the  $C_1-C_{60}(CF_3)_2(CN)^-$  intermediate has the  $p^2$  addition pattern shown in Figure 8B, with other isomers, listed in Table 4, more than 13 kJ mol $^{-1}$  higher in energy. If true, this would indicate thermodynamic control for the nearly regiospecific addition of  $CN^-$  to **III**. Only the five lowest-energy isomers of  $C_{60}(CF_3)_2(CN)^-$  are listed in Table 4 (all 31 isomers were calculated; their relative energies range from 0.0 to 54.5 kJ mol $^{-1}$ ). Furthermore, it is easy to see from the LUMO diagram that the kinetically favored positions for the addition of a nucleophile like  $CN^-$  are C10, C11, and C28, if C8 ( $\Delta E(\text{anion}) = 36.6$  kJ mol $^{-1}$ ) is too sterically congested for facile cyanide addition (symmetry-related C atoms are omitted). Therefore, formation of the  $p^2$  intermediate shown in Figure 8B may be kinetically and thermodynamically favored.

Subsequent addition of the electrophiles  $CH_3^+$  or  $H^+$  led cleanly to only two isomers of  $C_{60}(CF_3)_2(CN)(X)$  in approximately 3:2 ( $X = CH_3$ ) or 1:1 ( $X = H$ ) molar ratios, respectively (Figure 8C,D). According to the ESP calculated for  $C_{60}(CF_3)_2(CN)^-$ , the most likely sites for electrophilic attack are the two C atoms, on a common pentagon, which are *ortho* to the cage C atoms bearing either the CN group or the terminal  $CF_3$  group. However, as shown in Figure 9 and in Table 4, electrophilic attack at these two sites led to *ortho-meta-para* (*omp*) products, for  $X = CH_3$ , that differ in



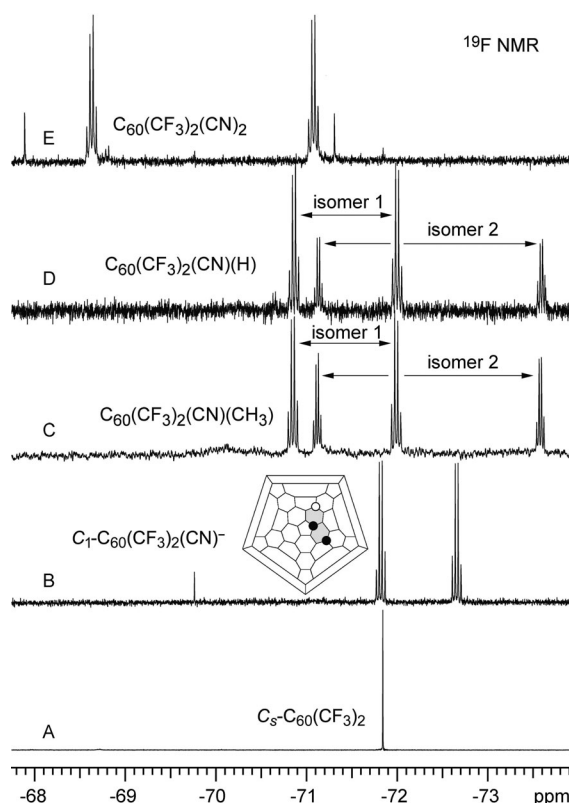


Figure 8.  $^{19}\text{F}$  NMR spectra (376.5 MHz;  $\text{CD}_2\text{Cl}_2$ ;  $\delta(\text{C}_6\text{F}_6) = -164.9$  ppm) showing A) the singlet of **III**, B) the two-quartet pattern of  $\text{C}_1\text{-C}_{60}\text{-(CF}_3)_2\text{(CN)}^-$ , the two-quartet patterns for the two predominant isomers of C)  $\text{C}_1\text{-C}_{60}\text{-(CF}_3)_2\text{(CN)(CH}_3\text{)}$  and D)  $\text{C}_1\text{-C}_{60}\text{-(CF}_3)_2\text{(CN)(H)}$ , and E) the two-quartet pattern for the predominant isomer of  $\text{C}_1\text{-C}_{60}\text{-(CF}_3)_2\text{(CN)}_2$ . A Schlegel diagram showing the DFT-predicted lowest-energy isomer of  $\text{C}_1\text{-C}_{60}\text{-(CF}_3)_2\text{(CN)}^-$  is also shown.

Table 4. DFT-predicted relative energies ( $\text{kJ mol}^{-1}$ ) of selected  $\text{C}_{60}\text{-(CF}_3)_2\text{(CN)}^-$  anions and neutral  $\text{C}_{60}\text{(CF}_3)_2\text{(CN)(X)}$  compounds ( $\text{X} = \text{CH}_3, \text{H, CN}$ ).<sup>[a]</sup>

CN locant	$\Delta E$ (anion)	X locant	$\Delta E$ (neutral)		
			$\text{CH}_3$	H	CN
11	0.0	10	0.0	0.0	0.0
11		8	19.1	0.4	9.4
11		27	19.2	32.1	14.5
11		24	21.7	33.2	15.3
28	13.4				
17	19.5	16			25.9
10	22.5				
15	24.7		119.4	99.0	
27	25.7	26			24.9

[a] The locants refer to the numbered Schlegel diagram in Figure 9.

relative energy by  $19.1 \text{ kJ mol}^{-1}$ . Furthermore, there are two  $p^3$  product isomers that are within  $2.6 \text{ kJ mol}^{-1}$  of the  $19.1 \text{ kJ mol}^{-1}$  *omp* product (also for  $\text{X} = \text{CH}_3$ ).

The effects of sterics on the relative stabilities of the  $\text{C}_{60}\text{-(CF}_3)_2\text{(CN)(X)}$  compositions was examined by calculating the  $\Delta E$  values for the  $\text{X} = \text{H}$  isomers. The  $p^3$  isomers are predicted to be less stable than the *omp* isomers by  $\geq 32 \text{ kJ mol}^{-1}$  for  $\text{X} = \text{H}$  but by only  $\leq 22 \text{ kJ mol}^{-1}$  for  $\text{X} = \text{CH}_3$ , and, significantly, the two *omp* isomers differ by only

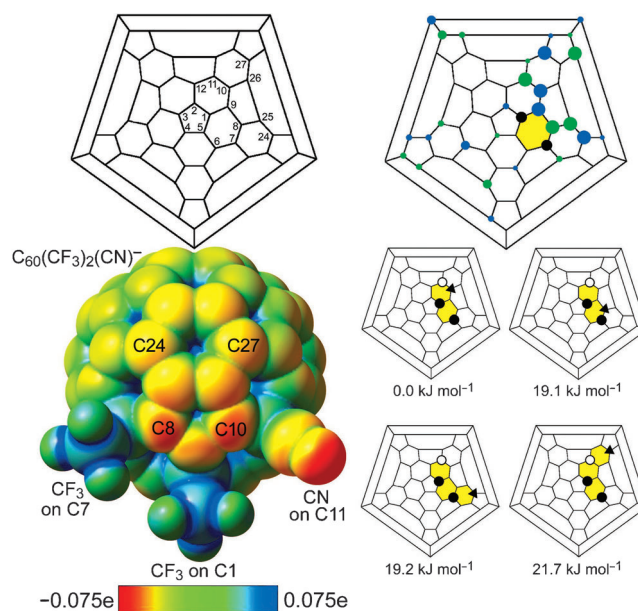


Figure 9. Schlegel diagrams showing the IUPAC numbering for  $\text{C}_{60}$  (top left), the DFT-predicted LUMO for  $\text{C}_5\text{-}p\text{-C}_{60}\text{-(CF}_3)_2$  (**III**, top right), a DFT-predicted ESP diagram for  $\text{C}_1\text{-C}_{60}\text{-(CF}_3)_2\text{(CN)}^-$ , and Schlegel diagrams for the lowest energy and most likely isomers of  $\text{C}_1\text{-C}_{60}\text{-(CF}_3)_2\text{(CN)-(CH}_3\text{)}$ .

$0.4 \text{ kJ mol}^{-1}$  for  $\text{X} = \text{H}$  but by  $19.1 \text{ kJ mol}^{-1}$  for  $\text{X} = \text{CH}_3$ . Therefore, for two reasons, we conclude that the electrophilic addition of  $\text{CH}_3^+$  or  $\text{H}^+$  to  $p^2\text{-C}_{60}\text{(CF}_3)_2\text{(CN)}^-$  may be under kinetic control: 1) for  $\text{X} = \text{CH}_3$  the DFT-predicted most stable isomer, nearly  $20 \text{ kJ mol}^{-1}$  more stable than the next most stable isomer, is not the only predominant isomer that is formed (it might not even be one of the predominant isomers) and 2) for  $\text{X} = \text{H}$  the same two predominant isomers appear to be formed (based on their  $^{19}\text{F}$  NMR spectra), in approximately the same relative amounts, despite the fact that the difference in energy for the two most stable isomers is less than  $1 \text{ kJ mol}^{-1}$  for  $\text{X} = \text{H}$  but  $19.1 \text{ kJ mol}^{-1}$  for  $\text{X} = \text{CH}_3$ .

An additional piece of relevant evidence is shown in the  $^{19}\text{F}$  NMR spectrum, shown in Figure 8E, produced by the addition of  $p\text{-TsCN}$  to  $\text{C}_{60}\text{(CF}_3)_2\text{(CN)}^-$ . Only one predominant isomer was formed, which is asymmetric, and one of the pairs of quartets has a very different  $\delta$  value than the quartets for either of the  $\text{X} = \text{CH}_3$  or  $\text{H}$  products (the spectrum in Figure 8E also exhibits two, much less intense, singlets, which will not be discussed further. If this is the  $\text{C}_{60}\text{-(CF}_3)_2\text{(10,11-CN)}_2$  isomer, then we must explain the absence of a second predominant isomer of this composition. If the predominant isomer is  $\text{C}_{60}\text{(CF}_3)_2\text{(11,27-CN)}_2$ , possibly for steric reasons because the electrophilic reagent  $p\text{-TsCN}$  is sterically more demanding than either  $\text{CH}_3\text{OTf}$  or  $\text{CF}_3\text{COOH}$ , then we must explain the absence of symmetric  $\text{C}_{60}\text{(CF}_3)_2\text{(11,24-CN)}_2$  as a second predominant isomer, since the environment of C24 is sterically similar to that of C27. Our tentative hypothesis is that the electrophilic reagent is attracted to the site of greatest negative charge on the sur-

face of the  $C_{60}(CF_3)_2(11-CN)^-$  intermediate, which is the cyano group N atom, and from there the incipient electrophile adds to the closest, sterically accessible cage C atom with substantial negative charge, either C27 in the case of  $p$ -TsCN or both C10 and C27 in the case of either  $CH_3OTf$  or  $CF_3COOH$ . However, without confirmation by X-ray crystallography, we cannot, at this time, confidently predict the most likely addition patterns for the predominant isomers of  $C_{60}(CF_3)_2(CN)(CH_3)$ ,  $C_{60}(CF_3)_2(CN)(H)$ , or  $C_{60}(CF_3)_2(CN)_2$ .

## Conclusion

We have probed the predominant sites of anionic nucleophile addition to PFAFs **I**, **II**, and **III** and the predominant sites of subsequent cationic electrophile addition to the anionic PFAF-derived intermediates. When this study was conceived, we did not know if the electrophiles would simply remove the nucleophiles from the  $PFAF(Nu)_n^{n-}$  intermediates (e.g.,  $CH_3^+$  removing  $CN^-$  to irreversibly form  $CH_3CN$ ). As it turned out, they did not. For both types of addition, and with two nucleophiles and three electrophiles, the regioselectivity for the predominant isomer or pair of isomers was >50 mol % for  $C_{70}(CF_3)_{10}(CH_3)_2(CN)_2$  and 90+ mol % for the other reactions. In the case of **I**, the sites of nucleophilic and electrophilic attack are the symmetry-related cage C atoms that comprise the previously identified most reactive C=C bond. In the case of a single nucleophile addition to **II**, these sites also comprise the previously identified most reactive C=C bond, but our results demonstrate for the first time that only one of these two unique  $C(sp^2)$  atoms is, almost exclusively, the site of nucleophilic attack. In the case of a double nucleophile addition to **II**, one nucleophile was added to either of the two most reactive C=C bond  $C(sp^2)$  atoms and another nucleophile added to a  $C(sp^2)$  atom far removed from the first site, and “its” electrophile added to a  $C(sp^2)$  atom *para* to it and not to a neighboring C atom (i.e., the concept of a second-most-reactive C=C bond in **II** is invalid). In the case of **III**, the addition of the nucleophile/electrophile pairs led to one or two predominant isomers, at least one of which could not have been formed by addition to a cage C=C bond. The experimental results are supported by DFT calculations, which indicate that some of the electrophile additions may be kinetically controlled rather than thermodynamically controlled, but further work will be necessary to confirm this. Taken together, this work goes beyond the chemistry of PFAFs and suggests that the sequential one-pot addition of different types of substituents to specific cage C atoms of fullerene derivatives could lead to the design of even more elaborate derivatives by using DFT as a guide, instead of merely discovering new derivatives by trial and error.

## Experimental Section

**General information:** All reagents and solvents were reagent grade or better. The reagents  $NEt_4CN$ ,  $p$ -TsCN,  $CH_3OTf$ , and  $CF_3COOH$  were obtained from Sigma-Aldrich and were used as received. All solvents were dried by standard techniques and stored under purified dinitrogen. The PFAFs **I**, **II**, and **III** were prepared as previously described. All manipulations of  $PFAF(CN)^-$  solutions were carried out under an atmosphere of purified dinitrogen by using either glovebox or Schlenk techniques. HPLC analyses and purifications were carried out by using Shimadzu HPLC instrumentation (CBM-20A control module, SPD-20A UV detector set to 300 nm, LC-6AD pump, manual injector valve) equipped with a semi-preparative 10 mm I.D.  $\times$  250 mm or a preparative 25 mm I.D.  $\times$  250 mm Cosmosil Buckyprep column (Nacalai Tesque).  $^{19}F$  NMR spectra were recorded by using a Varian 400 spectrometer operating at 376.5 MHz ( $C_6F_6$  internal standard,  $\delta = -164.9$  ppm). Negative-ion APCI mass spectra (see the Supporting Information) were recorded by using a Finnigan 2000 LCQ-DUO spectrometer. The samples were injected as approximately 50:50 v/v  $PhCH_3/MeCN$  solutions; the mobile phase was MeCN. Electronic spectra (see the Supporting Information) were recorded by using a Cary 500 spectrophotometer with a resolution of 1 nm. X-ray diffraction data for a single crystal of  $C_{5-p}o(loop)-C_{70}(CF_3)_8(CN)_2$  were recorded by using synchrotron radiation at the Advanced Photon Source at the Argonne National Laboratory. X-ray diffraction data for a single crystal of  $C_{1-C_{70}}(CF_3)_{10}(33,44-CH_3)_2(23,34-CN)_2$  were recorded by using a Bruker Kappa APEX II CCD diffractometer at Colorado State University.

**Generation of  $NEt_4[C_{1-C_{70}}(CF_3)_8(CN)]$  in solution and the isolation of  $C_{5-p}$  and  $C_{1-C_{70}}(CF_3)_8(CN)_2$ :** In a typical preparation, the  $C_{1-C_{70}}(CF_3)_8(CN)^-$  anion was generated by adding an aliquot of a colorless solution of  $NEt_4CN$  (1.63 mL, 0.0104 mmol  $CN^-$ ) in MeCN (6.41 mm) to a yellow solution of **I** (9.67 mg, 0.00695 mmol) in  $PhCH_3$  (10 mL) at 23(2) °C ( $CN^-/I$  molar ratio = 1.50; in some preparations  $C_6D_6$  was used instead of  $PhCH_3$ ; **CAUTION!** salts of the cyanide anion are toxic and should be handled by trained personnel wearing protective clothing; any waste must be handled carefully, especially solutions to which acid has been added, because HCN is volatile and toxic). The reaction mixture became greyish-blue within seconds and remained the same color for 2 h, at which point an aliquot of a solution of  $p$ -TsCN in  $PhCH_3$  (9.40 mm) was added (7.20 mL, 0.0677 mmol “ $CN^+$ ”, 9.73 equiv based on **I**), creating a light-brown solution. After another 2 h, the solution was exposed to air, washed three times with water, and dried with  $MgSO_4$ . The solvent was removed under vacuum, leaving a yellow solid that was purified by HPLC analysis. See the Supporting Information for spectroscopic data other than the  $^{19}F$  NMR spectra shown in Figure 1.

**Generation of  $NEt_4[C_{1-C_{70}}(CF_3)_{10}(CN)]$  and  $C_{1-C_{70}}(CF_3)_{10}(CN)(H)$  in solution and the isolation of  $C_{1-C_{70}}(CF_3)_{10}(CN)(CH_3)$ :** In a typical preparation, the  $C_{70}(CF_3)_{10}(CN)^-$  anion was generated by adding an aliquot of a solution of  $NEt_4CN$  (3.04 mL, 0.0195 mmol  $CN^-$ ) in MeCN (6.41 mm) to a yellow solution of **II** (20.0 mg, 0.0131 mmol) in  $PhCH_3$  (10 mL) at 23(2) °C ( $CN^-/II$  molar ratio = 1.50; in some preparations  $C_6D_6$  was used instead of  $PhCH_3$ ). The reaction mixture became green within seconds and remained the same color for 1 day, at which point a large excess of  $CH_3OTf$  was added, instantly creating a yellow solution (**CAUTION!**  $CH_3OTf$  is volatile, toxic, and a suspected carcinogen and should only be handled by trained personnel wearing protective clothing). After 12 h, the solution was exposed to air, filtered through silica gel, and the solvent was removed under a flow of air. The remaining yellow solid was purified by HPLC analysis. At day 1, an NMR scale aliquot of the  $C_{70}(CF_3)_{10}(CN)^-$  anion was also quenched with a large excess of  $CF_3COOH$ , immediately creating a yellow solution. After 1 day, the solution was exposed to air, washed three times with water, and dried with  $MgSO_4$ . The solvent was removed and the remaining solid was purified by HPLC analysis. See the Supporting Information for spectroscopic data other than the Figure 6  $^{19}F$  NMR spectra.

**Generation of  $Li_2C_{70}(CF_3)_{10}(CH_3)_2$  as a green precipitate and the isolation of two isomers of  $C_{1-C_{70}}(CF_3)_{10}(CH_3)_2(CN)_2$ :** Four equivalents of  $LiCH_3$  in  $Et_2O$  were added to a yellow solution of **II** in toluene, causing

the immediate formation of a green precipitate and the disappearance of the  $^{19}\text{F}$  NMR multiplets belonging to **II**. Addition of four equivalents of *p*-TsCN resulted in the rapid formation of a golden-yellow solution and the complete disappearance of the precipitate. The reaction mixture was prepurified by flash chromatography to remove Li(*p*-Ts). The two predominant products were purified by HPLC analysis. The minor isomer afforded crystals suitable for X-ray diffraction.

**Generation of  $\text{NEt}_4[\text{C}_1\text{-C}_{60}(\text{CF}_3)_2(\text{CN})]$ , two isomers each of  $\text{C}_1\text{-C}_{60}(\text{CF}_3)_2(\text{CN})\text{-(CH}_3\text{)}$  and  $\text{C}_1\text{-C}_{60}(\text{CF}_3)_2(\text{CN})\text{H}$ , and a single isomer of  $\text{C}_1\text{-C}_{60}(\text{CF}_3)_2(\text{CN})_2$  in solution:** In a typical preparation, the  $\text{C}_{60}(\text{CF}_3)_2(\text{CN})^-$  anion was generated by adding an aliquot of a solution of  $\text{NEt}_4\text{CN}$  in  $\text{CH}_2\text{Cl}_2$  (11.4 mm, 0.11 mL, 0.0013 mmol,  $\text{CN}^-$ ) to a brown solution of **III** in  $\text{CD}_2\text{Cl}_2$  (1.1 mg, 0.0013 mmol) at 23(2) °C ( $\text{CN}^-/\text{III}$  molar ratio = 1.0). The reaction mixture became dark brown. After five min, NMR-scale aliquots were treated with an excess of  $\text{CH}_3\text{OTf}$ ,  $\text{CF}_3\text{COOH}$ , or *p*-TsCN. In all three cases, a yellow solution was formed immediately. These solutions were exposed to air, washed three times with water, and dried with  $\text{MgSO}_4$ . The solvent was removed and the remaining solids were purified by HPLC analysis. See the Supporting Information for spectroscopic data other than the  $^{19}\text{F}$  NMR spectra shown in Figure 8. Colorless solutions of  $\text{NEt}_4\text{CN}$  in  $\text{CH}_2\text{Cl}_2$  became yellow after 1 day; therefore fresh solutions were used for each reaction.

**DFT calculations:**<sup>[37–41]</sup> Optimizations of the molecular structures of all the species studied were performed at the PBE/TZ2P level by using the Priroda code. Expansion of electron density in an auxiliary basis set was used to accelerate the evaluation of Coulomb and exchange-correlation terms. Electrostatic potentials (ESPs) for optimized structures were computed at the B3LYP/6-311G\* level with the help of the program Firefly. The program ChemCraft was used to visualize ESP isosurfaces.

## Acknowledgements

We thank the Alexander von Humboldt Foundation, the Deutsche Forschungsgemeinschaft (PO1602/1-1), and the U.S. National Science Foundation (CHE-1012468) for financial support, Brian S. Newell for determining the structure of  $\text{C}_{70}(\text{CF}_3)_{10}(\text{CH}_3)_2(\text{CN})_2$ , and Prof. L. Dunsch for his continuing support. We thank U. Nitzsche for assistance with local computational resources at IFW Dresden and the Research Computing Center at Moscow State University for computing time on the SKIF-Chebyshev supercomputer. ChemMatCARS Sector15 is principally supported by the National Science Foundation/Department of Energy under Grant Number NSF/CHE-0822838. Use of the Advanced Photon Source was supported by the U.S. Department of Energy, Office of Science, Office of Basic Energy Sciences, under Contract No. DE-AC02-06CH11357.

- [1] A. Montellano López, A. Mateo-Alonso, M. Prato, *J. Mater. Chem.* **2011**, 21, 1305–1318.
- [2] O. V. Boltalina, I. V. Kuvychko, N. B. Shustova, S. H. Strauss in *Handbook of Carbon Nano Materials, Syntheses and Supramolecular Systems, Vol. 1* (Eds.: F. D'Souza, K. M. Kadish), World Scientific, Singapore, **2010**, pp. 101–143.
- [3] N. B. Shustova, I. V. Kuvychko, R. D. Bolskar, K. Seppelt, S. H. Strauss, A. A. Popov, O. V. Boltalina, *J. Am. Chem. Soc.* **2006**, 128, 15793–15798.
- [4] I. E. Kareev, A. A. Popov, I. V. Kuvychko, N. B. Shustova, S. F. Lebedkin, V. P. Bubnov, O. P. Anderson, K. Seppelt, S. H. Strauss, O. V. Boltalina, *J. Am. Chem. Soc.* **2008**, 130, 13471–13489.
- [5] S. I. Troyanov, N. B. Tamm, *Crystallogr. Rep.* **2009**, 54, 598–602.
- [6] S. I. Troyanov, N. B. Tamm, *Chem. Commun.* **2009**, 6035–6037.
- [7] S. I. Troyanov, N. B. Tamm, *Crystallogr. Rep.* **2010**, 55, 432–435.
- [8] N. B. Shustova, D. V. Peryshkov, I. V. Kuvychko, Y. S. Chen, M. A. Mackey, C. Coumbe, D. T. Heaps, B. S. Confait, T. Heine, J. P. Phillips, S. Stevenson, L. Dunsch, A. A. Popov, H. S. Steven, O. V. Boltalina, *J. Am. Chem. Soc.* **2011**, 133, 2672–2690.

- [9] N. B. Shustova, I. V. Kuvychko, A. A. Popov, M. von Delius, L. Dunsch, O. P. Anderson, A. Hirsch, S. H. Strauss, O. V. Boltalina, *Angew. Chem.* **2011**, 123, 5651–5654; *Angew. Chem. Int. Ed.* **2011**, 50, 5537–5540.
- [10] A. A. Popov, I. E. Kareev, N. B. Shustova, E. B. Stukalin, S. F. Lebedkin, K. Seppelt, S. H. Strauss, O. V. Boltalina, L. Dunsch, *J. Am. Chem. Soc.* **2007**, 129, 11551–11568.
- [11] I. V. Kuvychko, J. B. Whitaker, B. W. Larson, R. S. Raguindin, K. J. Suhr, S. H. Strauss, O. V. Boltalina, *J. Fluorine Chem.* **2011**, 132, 679–685.
- [12] N. Ovchinnikova, A. A. Goryunkov, P. A. Khavrel, V. A. Belov, M. G. Apenova, I. N. Ioffe, M. A. Yurovskaya, S. I. Troyanov, L. N. Sidorov, E. Kemnitz, *Dalton Trans.* **2011**, 40, 959–965.
- [13] N. S. Ovchinnikova, D. V. Ignat'eva, N. B. Tamm, S. M. Avdoshenko, A. A. Goryunkov, I. N. Ioffe, V. Y. Markov, S. I. Troyanov, L. N. Sidorov, M. A. Yurovskaya, E. Kemnitz, *New J. Chem.* **2008**, 32, 89–93.
- [14] Y. Takano, M. Á. Herranz, I. E. Kareev, S. H. Strauss, O. V. Boltalina, T. Akasaka, N. Martín, *J. Org. Chem.* **2009**, 74, 6902–6905.
- [15] Y. Takano, M. Á. Herranz, I. E. Kareev, S. H. Strauss, O. V. Boltalina, T. Akasaka, N. Martín, *Chem. Eur. J.* **2010**, 16, 5343–5353.
- [16] A. A. Goryunkov, N. A. Samokhvalova, P. A. Khavrel, V. A. Belov, V. Y. Markov, L. N. Sidorov, S. I. Troyanov, *New J. Chem.* **2011**, 35, 32–35.
- [17] S. I. Troyanov, E. Kemnitz, *Mendeleev Commun.* **2008**, 18, 27–28.
- [18] I. E. Kareev, I. V. Kuvychko, S. F. Lebedkin, S. M. Miller, O. P. Anderson, K. Seppelt, S. H. Strauss, O. V. Boltalina, *J. Am. Chem. Soc.* **2005**, 127, 8362–8375.
- [19] I. E. Kareev, G. Santiso-Quinones, I. V. Kuvychko, I. N. Ioffe, I. V. Goldt, S. F. Lebedkin, K. Seppelt, S. H. Strauss, O. V. Boltalina, *J. Am. Chem. Soc.* **2005**, 127, 11497–11504.
- [20] I. E. Kareev, I. V. Kuvychko, N. B. Shustova, S. F. Lebedkin, V. P. Bubnov, O. P. Anderson, A. A. Popov, S. H. Strauss, O. V. Boltalina, *Angew. Chem.* **2008**, 120, 6300–6303; *Angew. Chem. Int. Ed.* **2008**, 47, 6204–6207.
- [21] F. Diederich, R. Kessinger, *Acc. Chem. Res.* **1999**, 32, 537–545.
- [22] A. Hirsch, M. Brettreich, *Fullerenes—Chemistry and Reactions*, Wiley-VCH, Weinheim, **2005**.
- [23] C. Thilgen, F. Diederich, *Chem. Rev.* **2006**, 106, 5049–5135.
- [24] A. Herrmann, F. Diederich, C. Thilgen, H.-U. Termeer, W. H. Müller, *Helv. Chim. Acta* **1994**, 77, 1689–1706.
- [25] C. Thilgen, F. Diederich, *Top. Curr. Chem.* **1999**, 199, 135–171.
- [26] M. Keshavzar-K, B. Knight, G. Srdanov, F. Wudl, *J. Am. Chem. Soc.* **1995**, 117, 11371–11372.
- [27] B. Jousseme, G. Sonmez, F. Wudl, *J. Mater. Chem.* **2006**, 16, 3478–3482.
- [28] G. Khairallah, J. B. Peel, *Chem. Commun.* **1997**, 253–254.
- [29] G. Khairallah, J. B. Peel, *J. Phys. Chem. A* **1997**, 101, 6770–6774.
- [30] G. Khairallah, J. B. Peel, *Int. J. Mass Spectrom.* **2000**, 194, 115–120.
- [31] Crystal data for  $\text{C}_{80}\text{F}_{24}\text{N}_{22}(\text{CCl}_{2.32})$ :  $M_r = 1633.42 \text{ g mol}^{-1}$ ; orthorhombic;  $Pbcm$ ;  $a = 11.271(1)$ ,  $b = 19.520(2)$ ,  $c = 26.346(3) \text{ Å}$ ;  $V = 5796(1) \text{ Å}^3$ ;  $Z = 4$ ;  $T = 100(2) \text{ K}$ ; 6130 reflections; 4972 independent reflections; 576 parameters;  $R_1(I > 2\sigma(I)) = 0.0781$ ;  $wR_2 = 0.1971$ ; synchrotron radiation at ChemMatCARS Sector 15-B at the Advanced Photon Source at Argonne National Laboratory (diamond (111) crystal monochromator;  $\lambda = 0.41328 \text{ Å}$ ). A semi-empirical absorption correction was applied by using SADABS. The structure was refined by using SHELXTL. CCDC-814565 contains the supplementary crystallographic data for this paper. These data can be obtained free of charge from The Cambridge Crystallographic Data Centre via [www.ccdc.cam.ac.uk/data\\_request/cif](http://www.ccdc.cam.ac.uk/data_request/cif).
- [32] S. I. Troyanov, A. A. Popov, N. I. Denisenko, O. V. Boltalina, L. N. Sidorov, E. Kemnitz, *Angew. Chem.* **2003**, 115, 2497–2500; *Angew. Chem. Int. Ed.* **2003**, 42, 2395–2398.
- [33] A. A. Popov, I. E. Kareev, N. B. Shustova, S. F. Lebedkin, S. H. Strauss, O. V. Boltalina, L. Dunsch, *Chem. Eur. J.* **2008**, 14, 107–121.
- [34] Z. Xiao, F. D. Wang, S. H. Huang, L. B. Gan, J. Zhou, G. Yuan, M. J. Lu, J. Q. Pan, *J. Org. Chem.* **2005**, 70, 2060–2066.

- [35] I. E. Kareev, I. V. Kuvychko, A. A. Popov, S. F. Lebedkin, S. M. Miller, O. P. Anderson, S. H. Strauss, O. V. Boltalina, *Angew. Chem.* **2005**, *117*, 8198–8201; *Angew. Chem. Int. Ed.* **2005**, *44*, 7984–7987.
- [36] Crystal data for  $C_{85}H_8Cl_2F_{30}N_2$ :  $M_r = 1697.83 \text{ g mol}^{-1}$ ; triclinic;  $P\bar{1}$ ;  $a = 12.7507(16)$ ,  $b = 12.7605(17)$ ,  $c = 19.956(2) \text{ \AA}$ ;  $\alpha = 81.693(7)$ ,  $\beta = 81.333(6)$ ,  $\gamma = 89.437(7)^\circ$ ;  $V = 3175.9(7) \text{ \AA}^3$ ;  $Z = 2$ ;  $T = 120(2) \text{ K}$ ; 5408 reflections; 3876 independent reflections; 656 parameters;  $R_1(I > 2\sigma(I)) = 0.0767$ ;  $wR_2 = 0.2075$ ; Bruker Kappa APEX II CCD diffractometer ( $Mo_{K\alpha}$ ,  $\lambda = 0.71073 \text{ \AA}$ ; graphite monochromator). A semi-empirical absorption correction was applied by using SADABS. The structure was refined by using SHELXTL. CCDC-902699 contains the supplementary crystallographic data for this paper. These data can be obtained free of charge from The Cambridge Crystallographic Data Centre via [www.ccdc.cam.ac.uk/data\\_request/cif](http://www.ccdc.cam.ac.uk/data_request/cif).
- [37] J. P. Perdew, K. Burke, M. Ernzerhof, *Phys. Rev. Lett.* **1996**, *77*, 3865–3868.
- [38] D. N. Laikov, Y. A. Ustynuk, *Russ. Chem. Bull.* **2005**, *54*, 820–826.
- [39] D. N. Laikov, *Chem. Phys. Lett.* **1997**, *281*, 151–156.
- [40] A. A. Granovsky, Firefly version 7.1.G, <http://classic.chem.msu.su/gran/gamess/index.html>.
- [41] M. W. Schmidt, K. K. Baldridge, J. A. Boatz, S. T. Elbert, M. S. Gordon, J. H. Jensen, S. Koseki, N. Matsunaga, K. A. Nguyen, S. Su, T. L. Windus, M. Dupuis, J. A. Montgomery, *J. Comput. Chem.* **1993**, *14*, 1347–1363.

Received: October 8, 2012


Revised: November 24, 2012

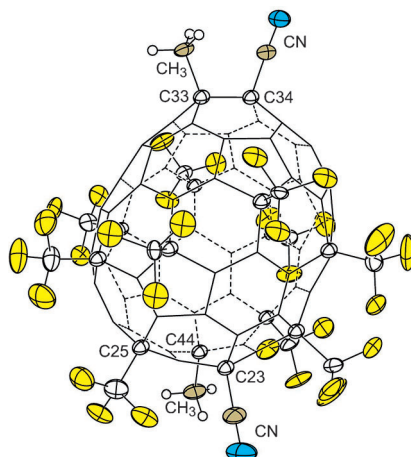
Published online: ■■■■, 0000



**Coordination Chemistry**

T. T. Clikeman, I. V. Kuvychko,  
N. B. Shustova, Y.-S. Chen,  
A. A. Popov,\* O. V. Boltalina,\*  
S. H. Strauss\* ..... ■■■■-■■■■

 **Regioselective Sequential Additions of Nucleophiles and Electrophiles to Perfluoroalkylfullerenes: Which Cage C Atoms Are the Most Reactive and Why?**



**Regioselective sequential additions** of  $\text{CH}_3^-$  or  $\text{CN}^-$  and the electrophiles  $\text{CH}_3^+$ ,  $\text{H}^+$ , or  $\text{CN}^+$  are reported for three perfluoroalkylfullerenes,  $p\text{-C}_{60}(\text{CF}_3)_2$ ,  $\text{C}_s\text{-C}_{70}(\text{CF}_3)_8$ , and  $\text{C}_{1\text{-}C_{70}}(\text{CF}_3)_{10}$ , including the structures of  $\text{C}_s\text{-}p^9o\text{-(loop)-C}_{70}(\text{CF}_3)_8(\text{CN})_2$  and  $\text{C}_{70}(\text{CF}_3)_{10}(\text{CH}_3)_2(\text{CN})_2$  (see figure).